values discriminate sharply against solutions other than YLAN3M.

ACKNOWLEDGMENTS

Especial thanks are due to Dr. P. M. Patel and Dr. A. S. Carroll for great assistance during the early stages of this work.

APPENDIX

It is perhaps worthwhile to point out why this measurement was made at 170° rather than 180°. For an ideal geometry of point targets and point detectors, the second scattering plane is undefined at $\theta_2=180°$, and experiments measuring the parameters D_t and R_t' become operationally indistinguishable. While such an experiment with an ideal geometry could be interpreted easily enough, it cannot be readily interpreted with finite angular resolutions such as ours. 170° was therefore chosen for being close enough to 180° to be significant in terms of the phase shift solutions, yet representing a lab angle large enough to define the second scattering plane satisfactorily.

PHYSICAL REVIEW VOLUME 134, NUMBER 3B 11 MAY 1964

Differential Cross Sections for Triton-Induced Reactions on N^{14}

R. B. SCHWARTZ,* H. D. HOLMGREN,† L. M. CAMERON, AND A. R. KNUDSON
Nucleonics Division, U. S. Naval Research Laboratory, Washington, D. C.
(Received 16 December 1963)

Differential cross sections have been measured as functions of angle and bombarding energy in the region from 1 to 2 MeV for the following reactions: (1) $N^{14}(t,t)N^{14}$; (2) $N^{14}(t,\alpha)C^{13}$ going to the ground state and the 3.09-MeV state in C^{13}; (3) $N^{14}(t,d)N^{15}$ going to the ground state of N^{15}; and (4) $N^{14}(t,p)N^{16}$ going to the ground state and the 0.120-, 0.295-, and 0.392-MeV states of N^{16}. The total cross sections for the last three of these reactions at 2 MeV are: (2) 11 and 6 mb; (3) 48 mb; and (4) 7, 4, 9, and 8 mb, respectively. The energy and angular behavior of the differential cross sections suggest that most of these reactions proceed predominantly by direct interactions. The large absolute value of the cross section for the $N^{14}(t,d_0)N^{15}$ reaction, as well as the energy and angular behavior of the differential cross section, suggest that this reaction may proceed by a cluster exchange process. Distorted-wave Born approximation (DWBA) calculations provide satisfactory fits to the (t,α_0) angular distribution, but not the (t,d_0). Plane-wave calculations including exchange stripping give more acceptable fits to the (t,d_0) data.

I. INTRODUCTION

THE fact that the mass-3 particles (He^3 and H^3) have binding energies intermediate between that of the deuteron and of the α particle has led to the suggestion that the interactions of these particles with nuclei might emphasize certain characteristics of reaction mechansims not exhibited by the interactions of other particles.[1] This, in turn, might also reveal some aspects of nuclear structure which are not easily probed by other particles. The experimental study of low-energy mass-3 induced reactions has indeed suggested that a relationship exists between the mechanism of a reaction and the structure of the nuclei involved.[1–4] These investigations have further demonstrated that many of these reactions seem to proceed predominantly by direct interaction even at bombarding energies below 2 MeV.[4] The mass-3 induced reactions also appear to be particularly sensitive to the apparent cluster nature of the nuclei involved.[4,5] These two phenomena will be discussed in more detail below in connection with the results obtained in the current investigation.

This paper is a report of an experimental study of the interactions of tritons with N^{14}, and a semiquantitative explanation of the significant features observed. We have measured differential cross sections as functions of angle and bombarding energy in the range between 1 and 2 MeV, for the following reactions: (1) $N^{14}(t,t)N^{14}$; (2) $N^{14}(t,\alpha)C^{13}$ going to the ground state and the 3.09-MeV state in C^{13}; (3) $N^{14}(t,d)N^{15}$ going to the ground state of N^{15}; and (4) $N^{14}(t,p)N^{16}$ going to the ground state and the 0.120-, 0.295-, and 0.392-MeV states of N^{16}. Alpha-particle groups corresponding to the combined 3.68- and 3.85-MeV levels and to the 6.87-MeV

* Present address: Nuclear Physics Branch, National Bureau of Standards, Washington, D. C.
† Present address: Physics Department, University of Maryland, College Park, Maryland.

[1] H. D. Holmgren, in *Proceedings of the International School of Physics "Enrico Fermi" XV Course*, edited by G. Racah (Academic Press Inc., New York, 1962), p. 223.
[2] R. Middleton, in *Proceedings of the International Symposium on Direct Interactions and Nuclear Reaction Mechanisms, Padua*, edited by E. Clementel and C. Villi (Gordon and Breach, New York, 1963), p. 435.
[3] D. A. Bromley, in *Proceedings of the International Conference on Nuclear Structure*, edited by D. A. Bromley and E. W. Vogt (University of Toronto Press, Toronto, 1960), p. 272.
[4] G. D. Gutsche, H. D. Holmgren, L. M. Cameron, and R. L. Johnston, Phys. Rev. **125**, 648 (1962).
[5] H. D. Holmgren and E. A. Wolicki, in *Proceedings of the Rutherford Jubilee International Conference, Manchester, 1961*, edited by J. B. Birks (Heywood and Company, Ltd., London, 1961), p. 541.

TABLE I. The columns labeled "E_{exc}" and "Q" are the final-state excitation energies and Q values, respectively, in MeV. J^{π} is the spin and parity for the final states. σ is the measured total cross section in mb for 1.98-MeV triton energy in the case of the (t,α) and (t,d) reactions and 1.8 MeV for the (t,p) reaction.

Reaction	E_{exc}	J^{π}	Q	σ
$N^{14}(t,t)N^{14}$	g.s.	1^+	0	···
$N^{14}(t,\alpha)C^{13}$	g.s.	$\frac{1}{2}^-$	12.26	11
	3.085	$\frac{1}{2}^+$	9.18	6
	3.680	$\frac{3}{2}^-$	8.58	13
	3.850	$\frac{5}{2}^+$	8.41	
	6.868	$\frac{5}{2}^+$	5.39	20
$N^{14}(t,p)N^{16}$	g.s.	2^-	4.85	7
	0.120	0^-	4.73	4
	0.295	3^-	4.55	9
	0.392	1^-	4.46	8
$N^{14}(t,d)N^{15}$	g.s.	$\frac{1}{2}^-$	4.58	48

level were observed to the extent that an estimate of their total cross section could be made. Table I lists the Q values, spins, and parities of the final states, and our measured total cross sections for all of the observed triton reactions on N^{14}. The energies, spins, and parities were all taken from a recent compilation.[6]

Preliminary reports of some of these data have been given previously.[7]

II. PROCEDURE

The triton beam from the Nucleonics Division 2-MV Van de Graaff accelerator was analyzed by a 90° magnet and focused onto the target through a set of collimators by an electrostatic lens.

Both solid and gaseous nitrogen targets were used during the course of the experiment. The solid targets were prepared by evaporating adenine ($C_5H_3N_4 \cdot NH_2$) onto a substrate material which acted as a getter. It was found that targets prepared without the use of a gettering material decomposed rapidly under beam bombardment. Titanium was chosen for the substrate, since it is the lowest Z material which is known to act as an effective getter for nitrogen, and hence has the lowest cross section for elastic scattering of the triton beam. (It was necessary to keep the number of elastically scattered tritons as small as possible in order to minimize pile-up at low angles.) Since attempts at making a thin, self-supporting titanium foil were unsuccessful, the targets were made by first preparing a thin carbon foil, then evaporating titanium onto the carbon, and finally evaporating adenine onto the titanium. These targets proved to be sufficiently stable to be used in the angular distribution measurements of the alphas and deuterons from the $N^{14}(t,\alpha)$ and $N^{14}(t,d)$ reactions. In these measurements slight target nonuniformity and instability could be tolerated since all data were normalized against a monitor counter at a fixed angle. These targets were, however, too unstable for the measurements of yield as a function of energy. For these yield curve measurements adenine was evaporated onto a 0.001-in.-thick tantalum foil. Such targets proved to be relatively uniform and stable. The tantalum was, however, too thick to permit α-particle measurements in the forward direction; hence α-particle yield curves were measured only for angles greater than 90°.

It was found that the α-particle groups from targets prepared on the carbon-titanium foils were considerably broader than the groups from the tantalum foil targets when the two targets gave approximately the same yield. This fact indicates that the nitrogen was diffused throughout the titanium layer. The resultant apparent energy spread of the beam in these targets was from 100 to 200 keV. Since the shapes of the angular distributions were not found to be strongly energy sensitive, this effective thickness did not seriously affect the angular-distribution data.

All measurements with the solid targets were performed in a reaction chamber with fixed exit ports at 15° intervals. A 200-μin. Ni absorber was used for measurements at the extreme forward angles in order to stop the elastically scattered tritons. This foil was thin enough so that the high-energy α particles and deuterons did not suffer undue straggling in passing through it.

Since the solid targets actually contain more carbon than nitrogen, and since the Q value for the prolific $C^{12}(t,p_0)C^{14}$ [4] reaction is very close to the Q values for the $N^{14}(t,p)$ reactions to the four lowest lying states of N^{16}, a gas target was used for all the $N^{14}(t,p)N^{16}$

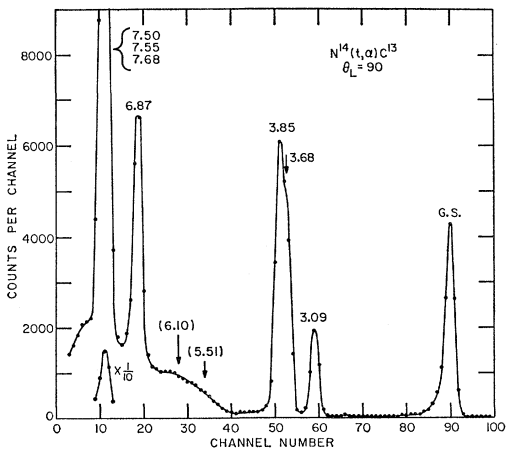

FIG. 1. Alpha-particle spectrum at 90° (lab) from the bombardment of a nitrogen gas target with 1.8-MeV tritons. Peaks are labeled with the excitation energies, in MeV, of the final states in C^{13}. Parentheses denote the calculated positions of peaks which were not observed. Data were taken with a surface-barrier detector having a depletion depth of 50 μ.

[6] F. Ajzenberg-Selove and T. Lauritsen, in *Landolt-Börnstein, Numerical Data and Functional Relationships in Science and Technology* (Springer-Verlag, Berlin, 1961), New Series, Vol. 1/1.

[7] R. B. Schwartz, L. M. Cameron, and H. D. Holmgren, Bull. Am. Phys. Soc. **6**, 416 (1961); L. M. Cameron, H. D. Holmgren, and R. B. Schwartz, *ibid.* **6**, 416 (1961); R. B. Schwartz, L. M. Cameron, and H. D. Holmgren, *ibid.* **7**, 286 (1962).

measurements. This gas target consisted of a cylindrical gas cell, 1 in. diam×1 in. high, with a 40-μin. nickel window which permitted measurements at all angles of interest. The gas cell was mounted in a sliding seal reaction chamber[8] which allowed the angle of the detector to be varied continuously from 0° to 132°. A continuous-flow gas system was used in which the nitrogen (99.996% minimum purity[9]) passed through a liquid-nitrogen trap to freeze out any residual impurities (CO_2 in particular). A pressure of 50 mm Hg was used in the gas cell. With this target, no reaction products arising from any contaminants could be observed.

The gas target not only produced much cleaner spectra but also had a higher yield per given energy spread of the incident beam in the target than did the solid targets. Its use, however, placed two important limitations on the measurements: (1) The beam energy loss in the window and in the gas meant that at our maximum incident energy of 2.0 MeV, the triton energy in the center of the target was only about 1.8 MeV, and (2) the correction for the variation in effective target thickness with angle became rather uncertain for angles less than about 20°; hence measurements could not be made at the extreme forward angles.

Most of the data were taken with silicon-surface barrier detectors (50-μ depletion depth for the α-particle measurements and 300-μ depletion depth for the proton and deuteron measurements), and a low-noise integrating preamplifier and biased main amplifier.[10] In order to observe the deuterons emitted from the solid targets, however, it was necessary to use a dE/dx and E system to separate these deuterons from the protons arising from the $C^{12}(t,p_0)$ contaminant reactions. This counter system consisted of a thin-window, gas-filled proportional counter (operated at a pressure such that the deuterons lost about 300 keV of energy in the gas) followed by a 0.03-in.-thick CsI crystal mounted on a type 6292 photomultiplier.

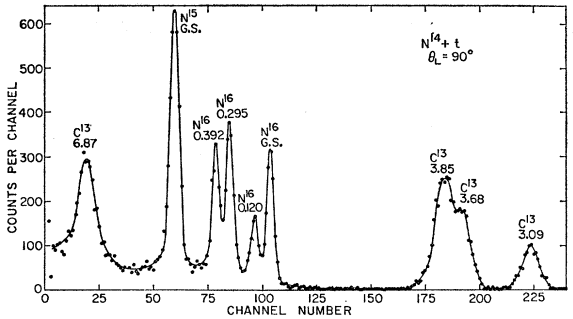

FIG. 2. Spectrum of alphas, protons, and deuterons taken at 90° (lab) with 1.8-MeV tritons. Peaks are labeled with the final nucleus and excitation energies of the final states. Data taken with a detector of 300-μ depletion depth.

[8] F. D. Loucks, Jr., Rev. Sci. Instr. **28**, 468 (1957).
[9] Matheson "Prepurified" grade.
[10] ORTEC Model 103-203, Oak Ridge Technical Enterprises Corporation.

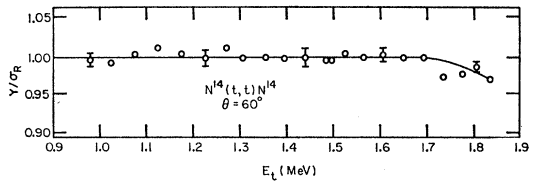

FIG. 3. The ratio of the elastic-scattering yield for tritons on N^{14} to the Rutherford cross section, at 60°.

III. RESULTS

Figures 1 and 2 are spectra taken at 90° with the gas target at a triton energy of 1.8 MeV at the center of the target. The data of Fig. 1 were taken using a detector with a 50-μ depletion depth; those of Fig. 2 were taken with a 300-μ detector. The latter was thick enough to stop the deuterons and protons, whereas these peaks are missing in the data taken with the 50-μ detector. This affords a very convenient method of particle identification.

The α-particle continuum starting below about channel 40 in Fig. 1 is due to either the two-step reaction $N^{14}(t,n)O^{16*}(\alpha)C^{12}$ or the three-body breakup reaction $N^{14}(t,n\alpha)C^{12}$.[11]

A. $N^{14}(t,t)N^{14}$

The yield of the elastically scattered tritons was measured at 60°, for energies between 0.98 and 1.83 MeV, using the gas target. The ratio of the experimental yields to the calculated Rutherford scattering cross section is shown in Fig. 3. The ratio is constant up to 1.7 MeV. This constant is assumed to be unity. The determination of the absolute cross sections for the rest of these experiments is based upon this assumption.

B. $N^{14}(t,\alpha)C^{13}$

All α-particle measurements except the determination of the absolute cross sections were made using the adenine targets. The energies given as the bombarding energy are the energies of the tritons incident on the target. Due to the effective thickness for the targets used in the angular-distribution measurements the average energy may be as much as 0.10 MeV less than this energy. Since the shapes of the angular distributions were not found to vary rapidly with energy, the angular distributions were normalized using the yield-curve data to obtain the correct absolute cross sections corresponding to the incident energy.

The differential cross sections for the ground state α-particle group from $N^{14}(t,\alpha)C^{13}$, measured at 15° intervals from 90 to 165°, are shown as functions of the bombarding energy in Fig. 4. The total cross section for this group increases rapidly with bombarding energy up to about 1.5 MeV and then tends to level off. The

[11] M. G. Silbert, Phys. Rev. **127**, 2113 (1962).

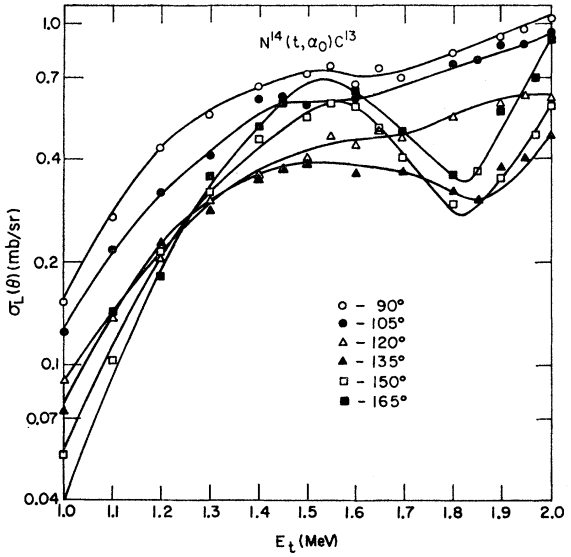

FIG. 4. Excitation curves for the $N^{14}(t,\alpha_0)C^{13}$ reaction at various laboratory angles.

135, 150, and 165° yield curves all show a broad minimum at about 1.82 MeV. Angular distributions for the ground-state group, measured at 1.25, 1.50, 1.78, and 1.98 MeV, are given in Fig. 5. The basic structure of these angular distributions is similar throughout most of the energy region studied, exhibiting a forward maximum (absent at the lowest bombarding energy), a secondary maximum at about 90°, a backward maximum, and minima at about 60 and 140°.

Angular distributions of the α-particles leading to the 3.09-MeV (first excited) state in C^{13} are given in Fig. 6, for bombarding energies of 1.50, 1.78, and 1.98 MeV. A noticeable feature of the curves is the slow increase in yield with increasing angle in the backward direction. Yield curves obtained at 135, 150, and 160° all show a simple monotonic increase with energy. This is shown in Fig. 7.

Although in some of the data the α-particle groups corresponding to the 3.68- and 3.85-MeV states in C^{13} are partially resolved (see Fig. 2), these groups were not resolvable in most of our runs; hence the only result that we present is the total cross section for the sum of the α-particle groups for these two states (Table I).

Levels in C^{13} at 5.51 and 6.10 MeV were reported by Moak *et al.*,[12] based on two weak proton groups from

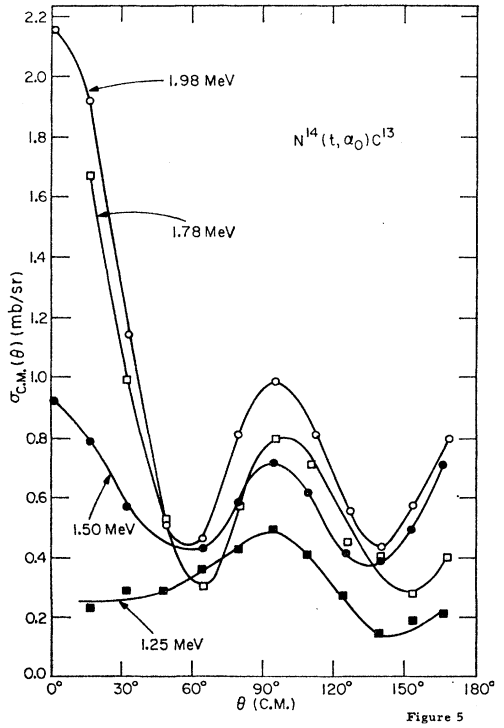

FIG. 5. Angular distributions for the $N^{14}(t,\alpha_0)C^{13}$ reaction at 1.98-, 1.78-, 1.50-, and 1.25-MeV triton energy.

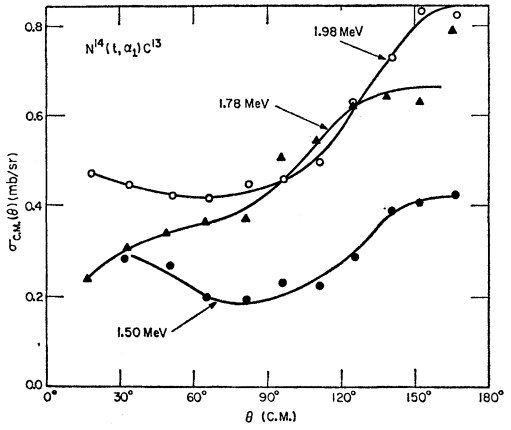

FIG 6. Angular distributions for the $N^{14}(t,\alpha_1)C^{13}$ reaction at 1.98-, 1.78-, and 1.50-MeV triton energy.

the $B^{11}(He^3,p)C^{13}$ reaction. Several other investigators[11,13,14] have since looked for these levels, with no success. Silbert[11] suggests that the proton groups observed by Moak *et al.* may have originated from the two-stage reaction $B^{11}(He^3,n)N^{13*}(p)C^{12}$, but, in any case, no evidence is found for the existence of these two levels in the present experiment. Groups corresponding to these levels would, for example, be expected to appear in channels 28 and 34 of Fig. 1. From the data of Fig. 1, we can conclude that the cross section for their formation, at 90°, at 1.8-MeV triton energy, is less than 3% of that for the formation of the ground-state group, i.e., less than 0.03 mb/sr. (We note that if

[12] C. D. Moak, A. Galonsky, R. L. Traughber, and C. M. Jones, Phys. Rev. **110**, 1369 (1958).

[13] A. Gallman, D. E. Alburger, D. H. Wilkinson, and F. Hibou, Phys. Rev. **129**, 1765 (1963).

[14] C. M. Huddleston, R. O. Lane, L. L. Lee, Jr., and F. P. Mooring, Phys. Rev. **117**, 1055 (1960).

these levels were very broad ($\Gamma > 150$ keV) we might not have observed them. Huddleston *et al.*,[14] however, were able to set an upper limit of $\Gamma < 300$ eV for these levels on the basis of neutron-transmission measurements.)

The α-particle group corresponding to the 6.87-MeV state of C^{13} could not be resolved with sufficient accuracy, when the solid targets were used, to allow reliable angular distributions to be obtained for this group. However, from the data with gas targets at one angle for several bombarding energies and from the rough data obtained with solid targets it was possible to estimate the total cross section for this group. The rough data at 1.98 MeV also indicate that the angular distribution for this group has a strong backward peak.

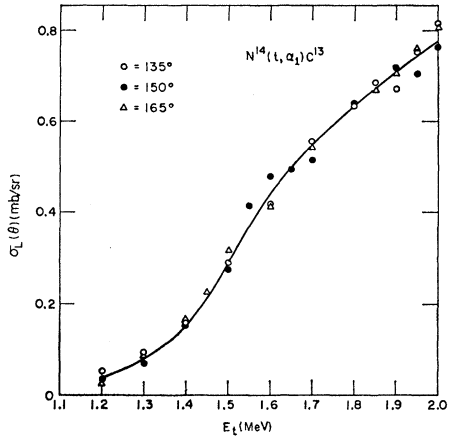

FIG. 7. Excitation curve for the $N^{14}(t,\alpha_1)C^{13}$ reaction. Differences among the data taken at the three angles are not considered significant; hence only one curve is drawn.

C. $N^{14}(t,d_0)N^{15}$

Deuteron yield curves from a tantalum-adenine target obtained with the dE/dx and E counter system are shown in Fig. 8. These curves show a rapid increase in yield with increasing bombarding energy; however they appear to be starting to level off at about 1.9 MeV.

Angular distributions for the ground-state deuteron group are given in Fig. 9. The curves for 1.50- and 1.98-MeV bombarding energy were obtained from the carbon-titanium-adenine target with the dE/dx and E counter system. The 1.83-MeV curve was taken using the gas target and surface-barrier detector. Strong forward and backward peaks are observed at all three bombarding energies; however, the minimum in the yield tends to shift slightly towards lower angles with increasing bombarding energy. Although no angular distribution was obtained at energies below 1.50 MeV for this group, the yield curves (Fig. 8) indicate that these two features of the angular distribution persist down to at least 1.20 MeV.

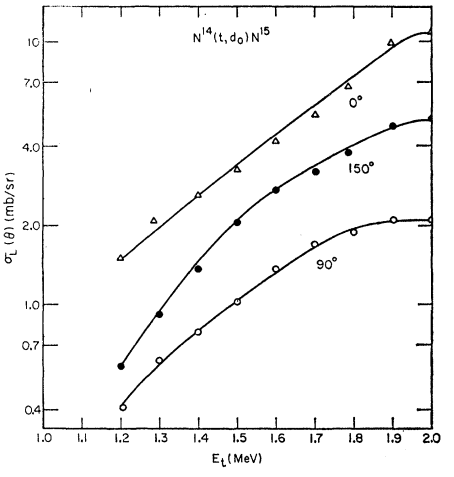

FIG. 8. Excitation curves for the $N^{14}(t,d_0)N^{15}$ reaction at laboratory angles 0, 90, and 150°.

D. $N^{14}(t,p)N^{16}$

All the proton data were taken with the gas target and a 300-μ depletion-depth surface-barrier detector.

The yield curves for proton groups corresponding to the ground state and first three excited states ($E_{exc}=0.120$, 0.295, and 0.392 MeV), obtained at 90° are shown in Fig. 10. These curves all tend to show an increase in cross section with increasing bombarding energy, although in detail their individual behaviors are different. The yield for the ground-state proton group appears to have reached a constant value above 1.55 MeV, while the yield at 90° for the first excited state group is almost constant from 1.30 to 1.55 MeV and then increases rapidly. The 90° yield of the p_2 group increases throughout the energy range studied

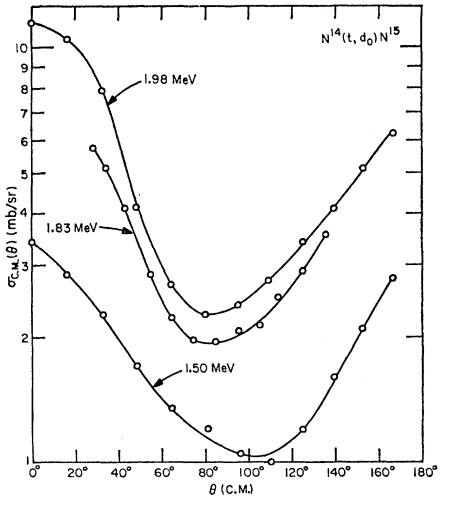

FIG. 9. Angular distributions for the $N^{14}(t,d_0)N^{15}$ reaction at 1.98-, 1.83-, and 1.50-MeV triton energy.

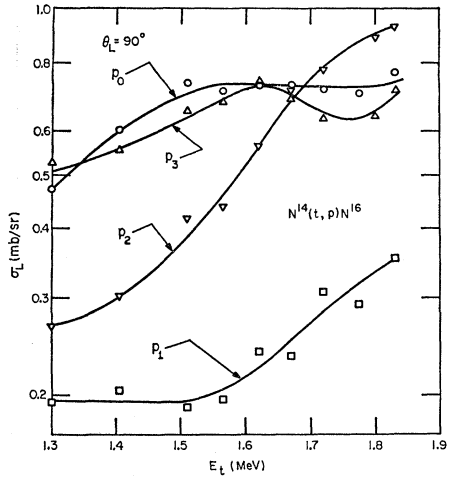

FIG. 10. Excitation curves for the $N^{14}(t,p)N^{16}$ reaction going to the ground state and first three excited states of N^{16}.

and that for the p_3 group shows a broad minimum near 1.75 MeV.

The angular distributions at 1.83 MeV for the four proton groups are shown in Fig. 11. The angular distributions of the protons leading to the ground state and second excited state of N^{16} show minima in the forward direction, while the first and third excited state groups show weak maxima at about 45°.

It should be noted that at small angles the counting rates of elastically scattered tritons were so high that pile-up in the amplifier (double delay-line clipped) distorted the spectrum to such an extent that it became increasingly difficult to resolve the proton groups. The usual procedure of stopping the scattered tritons with an absorber could not be used, since the straggling introduced by such an absorber caused too great a broadening of the proton groups to allow them to be resolved. Hence, reliable angular distributions could not be obtained for the protons emitted at angles less than 25°.

E. Absolute Cross Sections

Absolute cross sections were determined by comparison with the Rutherford scattering cross section, as indicated above. The total cross sections are listed in Table I, and were obtained by numerical integration under the appropriate angular distribution curves. The values listed are for 1.98-MeV triton energy in the case of the (t,α) and (t,d) reactions and 1.8-MeV for the (t,p) reactions.[15]

F. Errors

The elastic-scattering data are probably accurate to within 1% on the basis of counting statistics and reproducibility. (The error bars in Fig. 3 represent counting statistics only, but the reproducibility was of the same order.)

The relative values for the alpha and deuteron data are accurate to within 5%, but 10% errors are assigned to the proton data. The larger errors in the proton data arise from the uncertainties in subtracting the alpha background, which in turn is complicated by the imperfect resolution.

The absolute cross sections for the alphas and deuterons are accurate to within 10%, with the exception of the α-particle group corresponding to the 6.87-MeV state of C^{13} which is estimated to be accurate to within 25%. The absolute cross sections for the proton data are accurate to within 20%.

IV. DISCUSSION

As previously pointed out, most of the yield curves (Figs. 4, 7, 8, and 10) show relatively smooth increases with increasing energy, although the curves for the α_0 group at large angles exhibit broad minima in the vicinity of 1.8 MeV (Fig. 4). A similar behavior is observed in the yield of the p_3 group at 90° (Fig. 10). The gross structure of all these curves, however, seems to be determined primarily by the penetration of the Coulomb barrier. The minima observed near 1.8 MeV suggest some sort of interference phenomena; however no evidence is seen for any typical compound nucleus resonances. The elastic scattering at 60° (Fig. 3) appears to be essentially Rutherford scattering, again except for a possible anomaly at 1.8 MeV, where the cross section dips slightly below the Rutherford value.

In general the angular distributions change relatively slowly with energy and appear to retain their basic characteristics throughout most of the energy interval studied (Figs. 5, 6, and 9). This behavior, combined with observed lack of symmetry about 90°, is rather strong evidence that the dominant mode of interaction for these reactions is a direct process, although, of course, some compound nucleus formation

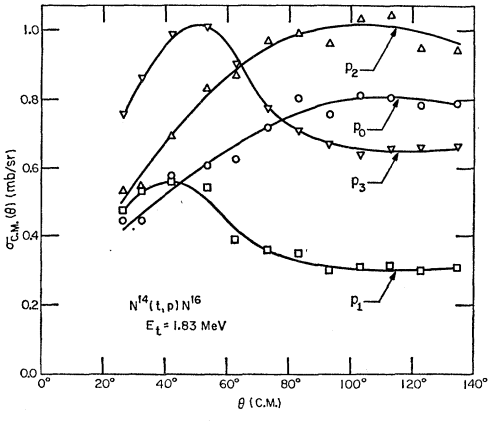

FIG. 11. Angular distributions for the $N^{14}(t,p)N^{16}$ reactions.

[15] We wish to point out that the total cross sections previously reported by us (Ref. 7) were all in error, due to incorrect normalizations.

TABLE II. DWBA parameters. Parameters used in generating the DWBA fits to the (t,α) and (t,d) data shown in Figs. 12, 13, and 14. V and W are the real and imaginary parts, respectively, of the Woods-Saxon potential. R_0 is the radius parameter (i.e., $r=R_0A^{1/3}$) and a is the surface diffuseness of the potential well. R_c is the radius parameter for the charge distribution. LCR is the lower cut-off radius, and R_N is the radius at which the harmonic-oscillator bound-state wave functions are matched to the exponentially decaying Coulomb functions. All energies are in MeV and lengths in fermis.

Curve	E	Particle	R_N	LCR	V	W	R_0	R_c	a
I	1.95	triton	3	3.17	55	55	1.6	1.6	0.65
		α			30	12	1.7	1.7	0.65
II	1.95	triton	3	3.68	35	8	1.8	1.5	0.60
		α			55	55	1.7	1.7	0.65
III	1.25	triton	3	3.00	55	55	1.6	1.6	0.65
		α			30	12	1.7	1.7	0.65
IV	1.25	triton	3	4.01	55	55	1.6	1.6	0.65
		α			30	12	1.7	1.7	0.65
V	1.25	triton	3	5.03	55	55	1.6	1.6	0.65
		α			30	12	1.7	1.7	0.65
VI	1.98	triton	3	0	35	8	1.85	1.5	0.60
		deuteron			50	30	1.5	1.5	0.65

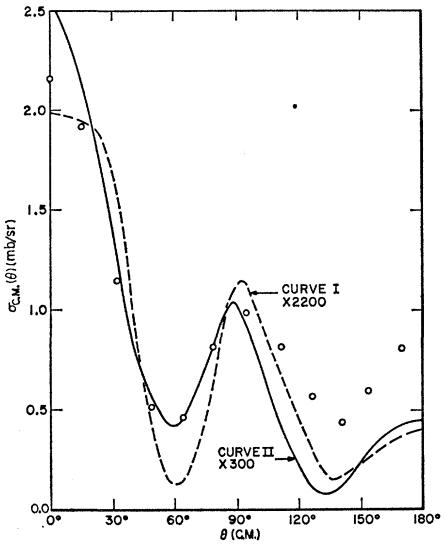

FIG. 12. Distorted-wave Born approximation fits to the $N^{14}(t,\alpha_0)C^{13}$ data. The circles are the 1.98-MeV data of Fig. 5. The parameters used are listed in Table II.

may also occur. The discussion which follows, however, will be from the direct interaction point of view.

A. $N^{14}(t,\alpha)C^{13}$

The angular distribution for the ground-state α-particle group (Fig. 5) shows no forward peak at the lowest energy (1.25 MeV). However, as the energy increases, a peak at forward angles appears and grows rapidly with increasing energy. The disappearance of the forward peak when the bombarding energy is well below the Coulomb barrier (Coulomb barrier energy $\approx$1.9 MeV) has been observed in a number of stripping reactions,[16] and may be due to Coulomb distortions. It was hoped that the DWBA calculations performed for this reaction would reproduce this behavior.

Figure 12 shows two fits to the 1.98-MeV (t,α_0) data, using the distorted-wave Born approximation (DWBA). The experimental points are the 1.98-MeV data of Fig. 5. The curves were calculated with the code "SALLY"[17] using the ORNL 704 computer. This code employs the so-called zero-range approximation for the interaction between the incident triton and the picked-up proton and neglects spin-orbit coupling. A Woods-Saxon potential was used for generating the optical-model wave functions, with parameters as given in Table II. The optical-model parameters of curve I are those suggested by Hodgson[18] extrapolated to light nuclei. Only a very limited variation of the optical-model parameters was made in order to attempt to improve the fit. Curve II represents another choice of the parameters. Several different values of the lower cutoff radius (LCR) and of the radius (R_N), at which the harmonic-oscillator bound-state wave functions are matched to the exponentially decaying Coulomb wave functions, were also tried. These were varied in rather large steps and no systematic effort was made to find the optimum values for either the optical-model parameters or the integration parameters. The curves have been arbitrarily normalized to the low-angle data. We note that the curves shown in Fig. 12 have maxima and minima at angles which are in approximate agreement with the data. It is felt that a more judicious choice of parameters might have brought the amplitudes of the calculated minima and secondary maxima into better agreement with the experimental data.

The absolute magnitudes of the cross section predicted by this theory for the sets of parameters used for curves I and II of Fig. 12 are, however, too small by factors of 2200 and 300, respectively. The satisfactory agreement in shape tends to indicate that the theory accounts for the kinematics of the interaction properly, although the nuclear structure aspects of the theory may be incorrect.

Figure 13 represents an attempt to fit the (t,α_0) data at 1.25 MeV using the same optical-model parameters as were used in curve I at 1.95 MeV. The calculated curves are plotted for three choices of the LCR; 3.00, 4.01, and 5.03 F. The parameters for these curves are also given in Table II. None of these curves resemble the experimental angular distribution, although it is possible that a calculation with a value of the LCR

[16] See, for example, D. H. Wilkinson, in *Proceedings of the International Conference on Nuclear Structure*, edited by D. A. Bromley and E. W. Vogt (University of Toronto Press, Toronto, 1960), p. 20.

[17] R. H. Bassel, R. M. Drisko, and G. R. Satchler, Oak Ridge National Laboratory Report ORNL-3240, 1962 (unpublished).

[18] P. E. Hodgson, in *Proceedings of the International Symposium on Direct Interactions and Nuclear Reaction Mechanisms, Padua*, edited by E. Clementel and C. Villi (Gordon and Breach, New York, 1963) p. 103.

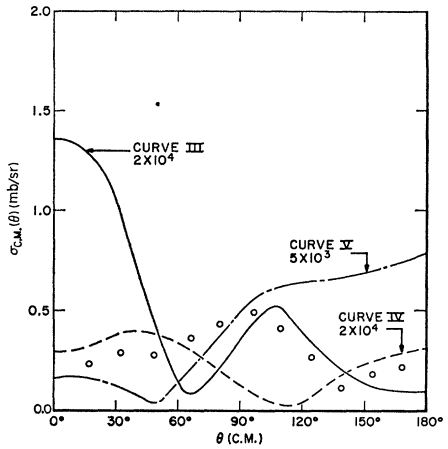

FIG. 13. Distorted-wave Born approximation fits to the $N^{14}(t,\alpha_0)C^{13}$ data at 1.25 MeV. The parameters used are listed in Table II.

between 4 and 5 F might produce an angular distribution similar to the experimental one.

It is particularly interesting to note that the 1.25-MeV calculations using the same optical-model parameters and approximately the same LCR which had previously given an acceptable fit to the 1.95-MeV data (Fig. 12, curve I) still indicate a substantial forward peak (Fig. 13, curve III), contrary to the experimental data. This may simply indicate the lack of applicability of the optical model to such a light nucleus, particularly at low bombarding energies.

In the case of the first-excited-state reaction (Fig. 6) the forward peak is missing at all bombarding energies, and not merely at the lowest energy. The absence of a forward peak in this case is probably not due to distortion effects, but rather to the fact that the direct pick-up reaction is l forbidden. That is, the shell-model configuration for the 1^+ ground state of N^{14} is primarily $(1p)^{10}$. The amount of $(1p)^8(2s)^2$ and $(1p)^8(2s)(1d)$ admixture is very small.[19] The first excited state of C^{13} is $\frac{1}{2}^+$, with a $(1p)^8(2s)$ configuration.[20] Hence, except for the very small $(1p)^8(2s)^2$ and $(1p)^8(2s)(1d)$ admixture in N^{14}, the $N^{14}(t,\alpha_1)C^{13*}$ reaction should be forbidden to proceed by pick-up with $l=0$ or $l=2$.

The first-excited-state reaction can proceed, however, via the heavy particle stripping mode, and the observed angular distributions (Fig. 6) are indeed typical of what may be expected for such a process[21]: no forward peak, a rather weak variation with angle, and a broad maximum in the backward direction.

Similar considerations may hold for the (t,α) reaction leading to the 6.87-MeV state in which a backward peak is also observed, except that in this case the final state is a $\frac{5}{2}^+$ level. (The data for this group are, however, rather uncertain and are not presented in this paper.)

B. $N^{14}(t,d_0)N^{15}$

The angular distributions for the $N^{14}(t,d_0)N^{15}$ reaction (Fig. 9) exhibit pronounced peaks in the backward as well as the forward directions. A forward peak is expected for either a stripping or knock-out reaction, while the backward peak suggests heavy-particle stripping.

Attempts to fit the 1.98-MeV angular distribution data using the DWBA[17] were unsuccessful. A typical result is shown in Fig. 14, and the appropriate parameters are listed in Table II. As in the case of the (t,α_0) DWBA fit no systematic attempt was made to find the best parameters, but a sufficient number of different values of the optical-model parameters were tried to make it clear that the failure to fit the data is due to a more fundamental difficulty than an improper choice of parameters. The inclusion of a finite range interaction may improve the quality of the fit, but without actually performing such calculations this is only conjecture. On the other hand the plane-wave Born approximation (PWBA) calculations indicate that the inclusion of heavy-particle stripping significantly improves the quality of the fit.

The results of a PWBA calculation, based on the method of Owen, Madansky, and Edwards,[22] are also

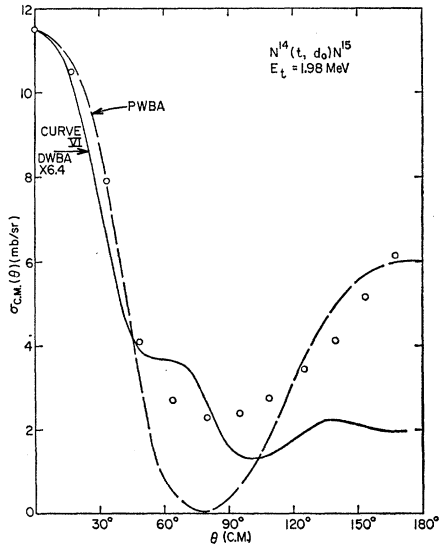

FIG. 14. DWBA and PWBA (including exchange) calculated fits to the $N^{14}(t,d_0)N^{15}$ data. The circles are the 1.98-MeV data of Fig. 9. The solid line is a curve computed with the code "SALLY" and the parameters of Table II. The dashed curve is the PWBA calculation, using the parameters indicated in Table III.

[19] K. G. Standing, Phys. Rev. **101**, 152 (1956); M. A. Nagarajan, Bull. Am. Phys. Soc. **7**, 559 (1962) and (private communication); W. W. True, Phys. Rev. **130**, 1525 (1963).

[20] I. Talmi and I. Unna, Ann. Rev. Nucl. Sci. **10**, 353 (1960).

[21] M. K. Bannerjee, in *Nuclear Spectroscopy*, edited by F. Ajzenberg-Selove (Academic Press, New York, 1960), Part B, p. 695, and private communication.

[22] G. E. Owen and L. Madansky, Phys. Rev. **105**, 1766 (1957); S. Edwards, Lectures on the Theory of Direct Reactions, notes by K. L. Warsh, Florida State University, Tandem Van de Graaff Laboratory, Tallahassee, 1961 (unpublished); G. E. Owen, L. Madansky, S. Edwards, Phys. Rev. **113**, 1575 (1959).

TABLE III. Parameters used in the PWBA calculations for the $N^{14}(t,d)N^{15}$ reaction. The first set of parameters corresponds to the PWBA curve in Fig. 14. The second set produced an almost identical curve. Λ_2/Λ_1 is the ratio of the heavy-particle stripping amplitude to the triton-stripping amplitude. R_i and l_i are the cut-off radius and orbital angular momentum, respectively, for ($i=1$) the neutron-deuteron, ($i=2$) the neutron $-N^{14}$, ($i=3$) deuteron $-C^{12}$, and ($i=4$) triton $-C^{12}$.

i	1	2	3	4
R_i(F)	2.56	4.43	6.81	4.40
l_i	0	1	2	1
$\Lambda_2/\Lambda_1=136$				
R_i(F)	3.10	4.16	3.41	3.93
l_i	0	1	0	1
$\Lambda_2/\Lambda_1=9.81$				

shown in Fig. 14. In these calculations the reaction is assumed to proceed by direct- and heavy-particle stripping. The values used for the adjustable parameters in this calculation are given in Table III. The plane-wave calculation fits the experimental data satisfactorily at the forward and backward angles. The poor fit in the region from about 60 to 120° is probably due to the neglect of distortion effects.

The theoretical curve presented in Fig. 14 is calculated on the assumption that the ground state of N^{14} is a ^3D state, i.e., $l_{d-C^{12}}=2$.[23,24] It was found possible to obtain a theoretical angular distribution almost identical to the one presented, by assuming the N^{14} ground state to be a ^3S state and using quite different values for Λ_2/Λ_1, and the four cut-off radii. Therefore, the fit presented in Fig. 14 does not constitute experimental evidence for a ^3D ground state in N^{14}. In view of this result, the possibility of using PWBA calculations to obtain information on the orbital angular momenta involved in a reaction proceeding by both direct- and heavy-particle stripping, is open to question.

The calculations indicate that, for a particular set of l values, the cutoff radii could not be changed significantly without seriously decreasing the quality of the fit, but that the value Λ_2/Λ_1, the ratio of the heavy-particle stripping amplitude to the triton-stripping amplitude, is not unique. This parameter could be varied by about a factor of 2 in either direction and very small changes in the radii would essentially restore the quality of the fit. For this reason, and because distortions would probably affect the magnitude of the direct stripping and heavy-particle stripping differently, any interpretation of the magnitude of Λ_2/Λ_1 in terms of, say, cluster configurations in N^{14} and N^{15} must be qualitative at best.

Although a stripping mechanism was used in the PWBA calculation to produce the forward peak, it is expected that in this reaction a knock-out calculation using slightly different interaction radii would produce results indistinguishable from those of the stripping mechanism.

[23] D. R. Inglis, Phys. Rev. **126**, 1789 (1962).
[24] B. G. Harvey and J. Cerny, Phys. Rev. **120**, 2162 (1960).

It is interesting to note that in the case of the $N^{14}(t,d_0)N^{15}$ reaction, the relative intensity of the forward peak is approximately the same at 1.50 MeV as it is at 1.98 MeV. The yield curves (Fig. 8) indicate that the large relative forward maximum persists well below the Coulomb barrier down to 1.2 MeV, in contract to the $N^{14}(t,\alpha_0)C^{13}$ reaction where the forward peak disappears below the Coulomb barrier. These two types of contrasting behavior have been observed in other mass-3 induced reactions and may be associated with the nature of the reaction mechanism, although this relationship is not understood.

The total cross section for the $N^{14}(t,d_0)N^{15}$ reaction is the largest observed for the $N^{14}+t$ reactions reported herein (see Table I). Inglis has shown[23] that the $(p_{1/2})^2$ configuration for N^{14} can give rise to a cluster structure which looks like a deuteron moving outside a C^{12} core. The cluster model also predicts such a structure,[25] as well as large-reaction cross sections when the initial- and final-state parentages are the same.[26] That is, cluster-exchange reactions should have large yields. Since knock-out and heavy-particle stripping are forms of cluster exchange, the cluster-exchange mechanism qualitatively accounts for both the strong forward and backward peak in the angular distributions, as well as the large cross section.

It has been pointed out[27,28] that the angular distributions of many (t,d) reactions which appear to proceed by stripping bear a marked similarity to the (d,p) reaction connecting the same pair of states. In this connection, it is of interest to examine some of the recent results of Kawai[29] who measured the angular distributions for the $N^{14}(d,p)N^{15}$ reaction at several different deuteron energies between 1.4 and 2.7 MeV. We find that Kawai's distributions for energies below 2.6 MeV are, indeed, similar to the (t,d) angular distributions reported here. We note, however, that (d,p) and (t,d) angular distributions should be similar only where the reaction proceeds by Butler stripping, and with no exchange effects.[28] Since we have indicated that exchange interactions probably play important roles in the $N^{14}(t,d)$ reaction, the reason for the similarity between the $N^{14}(d,p)$ and $N^{14}(t,d)$ data is not at all clear. Also the distortion effects would be expected to affect the two reactions quite differently.

C. $N^{14}(t,p)N^{16}$

The dominant shell-model configurations predicted by Elliott and Flowers[30] for the four lowest lying levels

[25] K. Wildermuth (private communication).
[26] G. C. Phillips and T. A. Tombrello, Nucl. Phys. **19**, 555 (1960).
[27] F. de S. Barros, P. D. Forsyth, A. A. Jaffe, and I. J. Taylor, Proc. Phys. Soc. (London) **77**, 853 (1961).
[28] P. D. Forsyth, F. de S. Barros, A. A. Jaffe, I. J. Taylor, and S. Ramavataram, Proc. Phys. Soc. (London) **75**, 291 (1960).
[29] N. Kawai, J. Phys. Soc. Japan **16**, 157 (1961).
[30] J. P. Elliott and B. H. Flowers, Proc. Roy. Soc. (London) **A242**, 57 (1957).

TABLE IV. The columns labeled "E_{exc}" and "J^{π}" are the energies of excitation and the spins and parities, respectively, for the four lowest lying levels of N^{16}. The column labeled "configuration" gives the dominant shell-model configuration of these states predicted by Elliott and Flowers.[a]

E_{exc}(MeV)	J^{π}	Configuration
g.s.	2^-	$p_{1/2}^{-1}d_{5/2}$
0.120	0^-	$p_{1/2}^{-1}s_{1/2}$
0.295	3^-	$p_{1/2}^{-1}d_{5/2}$
0.392	1^-	$p_{1/2}^{-1}s_{1/2}$

[a] See Ref. 30.

of N^{16} are given in Table IV. Considering $N^{14}(t,p)N^{16}$ as a stripping reaction, the two neutrons which are stripped from the triton must be uncoupled,[27] with one filling the (neutron) $1p$ shell, and the other starting the $2s$-$1d$ shell. It is of interest to see whether such a reaction is inhibited. The results listed in Table I show that although these cross sections are not particularly large, they do not seem to be very highly inhibited compared to the other reactions.

It should be noted that the ground-state and second-excited-state reactions may proceed with angular momentum transfers of $L=3$, while the first and the third excited states require $L=1$. The p_0 and p_2 angular distributions do, indeed, have generally similar shapes, as do the p_1 and p_3 distributions (Fig. 11).

V. CONCLUSIONS

It seems clear that the reactions described here proceed primarily by a direct interaction mechanism, even at energies as low as 1.2 MeV.

Qualitatively, the predictions of the cluster model seem to be borne out by both the shape and magnitude of the (t,d_0) angular distributions.

A PWBA fit to the (t,d_0) data is reasonably satisfactory, in view of the known shortcomings of plane-wave theories. The failure of the DWBA in the case of the (t,d_0) reaction suggests that inclusion of exchange stripping is necessary. The DWBA with the zero-range approximation gives quite a reasonable fit to the 1.95 MeV (t,α_0) angular distribution, although it fails to predict the proper magnitude of the cross sections. This may indicate that the formulation of the theory used for the present calculations gives the proper mechanism of the interaction but fails to take into account properly the structure of the nuclei.

ACKNOWLEDGMENTS

The authors wish to express their appreciation to Dr. G. R. Satchler for performing the DWBA calculations, as well as for many helpful discussions. We are also indebted to Dr. S. Meshkov for several interesting discussions. We wish to thank Dr. L. Cohen for his assistance during the course of the experiment, and V. W. Slivinsky for his help in taking the elastic-scattering data.

PHYSICAL REVIEW VOLUME 134, NUMBER 3B 11 MAY 1964

Differential Cross Sections for the Reaction $Li^7(Li^7,\alpha)Be^{10}$†

T. G. DZUBAY AND J. M. BLAIR
School of Physics, University of Minnesota, Minneapolis, Minnesota
(Received 2 December 1963)

Absolute differential cross sections are presented for the reaction $Li^7(Li^7,\alpha)Be^{10}$, where the Be^{10} is left in its ground state, first excited state, and combined second, third, and fourth excited states, for laboratory energies from 2.30 to 3.77 MeV. The total cross sections exhibit the rapid rise with increasing energy usually shown by heavy-ion reactions at low energies. The ratios of the coefficients of the Legendre polynomials which describe the angular distributions show structure in the neighborhood of 3.2-MeV bombarding energy. This is thought to be indicative of a compound-nucleus contribution.

INTRODUCTION

As a part of our program of investigation of reactions produced by lithium ions, we have previously[1–3] studied the angular distributions of alpha particles from C^{12} and Be^9 targets. In the present work we have extended these studies to the reaction $Li^7(Li^7,\alpha)Be^{10}$, where the residual Be^{10} nucleus was left in the ground and first four excited states. The alpha-particle groups leaving Be^{10} in its second, third, and fourth excited states could not be resolved, but were counted together. Lower energy groups of alpha particles could not be separated from a continuum, so no attempt was made to measure yield. The techniques described in the previous papers were used in this work, except that the target situation was more complicated, since self-supporting lithium foils could not be constructed.

† Supported in part by the U. S. Office of Naval Research.
[1] J. J. Leigh and J. M. Blair, Phys. Rev. **121**, 246 (1961).
[2] R. K. Hobbie, C. W. Lewis, and J. M. Blair, Phys. Rev. **124**, 506 (1961).
[3] R. K. Hobbie and F. F. Forbes, Phys. Rev. **126**, 2137 (1962).